Hydroxy-functionalized liquid crystalline polyazomethines II. Study of new central cores and synthesis of coordination polymers

J. Barbera; P. Cerrada; L. Oriol; M. Pinol; J. L. Serrano; P. J. Alonso

PLEASE SCROLL DOWN FOR ARTICLE

Hydroxy-functionalized liquid crystalline polyazomethines II. Study of new central cores and synthesis of coordination polymers

by J. BARBERÁ†, P. CERRADA†, L. ORIOL‡, M. PIÑOL‡, J. L. SERRANO*†
and P. J. ALONSO§

†Química Orgánica, Facultad de Ciencias,
Instituto de Ciencia de Materiales de Aragón (ICMA), Universidad de Zaragoza-
CSIC, Zaragoza 50009, Spain, ‡Química Orgánica,
Escuela Universitaria Politécnica de Huesca-ICMA, Universidad de Zaragoza-
CSIC, Ctra. Zaragoza s/n, Huesca 22071, Spain,
§Instituto de Ciencia de Materiales de Aragón (ICMA), Universidad de Zaragoza-
CSIC, Plaza S. Francisco s/n, Zaragoza 50009, Spain

A series of hydroxy-functionalized semi-flexible polyazomethines has been synthesized and characterized to investigate the effect of the structure of the diamine monomer on the thermal and mesogenic properties. The diamine monomer introduces structural modifications such as flexibility, lateral substitution, kinks or alteration of chain coaxiality. The mesomorphic phase of the mesogenic polymers was characterized as nematic in nature, but an evolution of the nematic into a smectic mesophase was observed for the polyazomethine derived from 3,3′-dimethoxybenzidine by annealing in the mesophase temperature range. Polyazomethines derived from aliphatic diamines were complexed with copper(II) to study the dependence of type of complexation on length of the aliphatic diamine.

1. Introduction

Polyazomethines or Schiff's base polymers, which contain –CH=N– bonds in their structure, may exhibit attractive physical properties such as electrical conductivity and optoelectronic, non-linear optical or excellent mechanical properties that provoke interest in such polymers in Materials Science. In particular, special attention has been paid to the study of electroactive and photoactive properties of aromatic polyazomethines [1] and the mechanical properties of high tensile strength, high modulus fibres obtained from the aromatic polyazomethines studied by DuPont's researchers [2]. Drawbacks of this kind of polymer are thermal intractability and insolubility in common organic solvents. Consequently, polymer characterization has to be carried out on solutions in strong protic solvents such as sulphuric acid, trifluoroacetic acid or methane sulphonic acid, which degrade the polymeric chains. However, Jenekhe and co-workers recently reported the solubilization of aromatic Schiff's base polymers in organic solvents via their soluble coordination complexes [3].

In a previous paper we reported the synthesis and the thermal and mesogenic properties of a series of hydroxy-functionalized semi-flexible polyazomethines [4]. The introduction of a hydroxyl group in the *ortho*-position to the azomethine bond leads to the formation of a strong chelate ring involving the nitrogen atom by means of hydrogen bonds, so improving the mesogenicity of the rigid core [5]. Furthermore, polyazomethines with hydroxyl groups react easily in the molten state giving rise to an increase in the degree of polymerization. Consequently, the properties of materials processed from the mesophase can be modified by controlling the thermal history. Thus, fibres of these polymers extruded from the nematic molten state exhibit good mechanical properties despite having a decamethylene flexible spacer which separates the mesogenic units [6]. In addition, fibres of these hydroxy-functionalized polyazomethines display a low tendency to fibrillate in comparison with fibres of liquid crystalline polyesters, probably due to intermolecular hydrogen bonds [7], or to the high electronic anisotropy and the resultant dipole associated with the H-chelate rings which give rise to high intermolecular interactions. Furthermore, the *ortho*-hydroxyl groups of such azomethines afford an exceptionally good way to capture some transition metals by complexation.
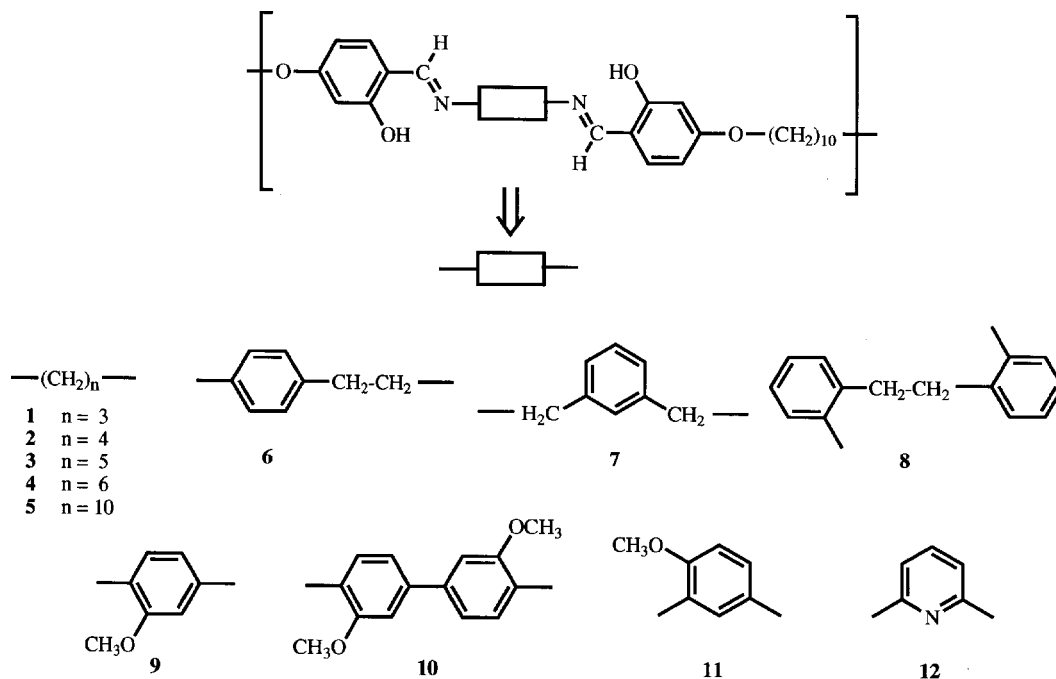
*Author for correspondence.

Figure 1. Schematic representation and nomenclature of the synthesized polyazomethines.

The possibility of introducing metals at specific points in the polymeric chains leads to polymers with interesting properties [8] such as conductivity [9], catalytic properties [10], magnetic [11] or non-linear optical properties [12]. The metal complexation of hydroxy-functionalized polyazomethines has been previously reported [13]. Apart from the properties associated with the presence of metal atoms, the introduction of para-magnetic entities, e.g. copper(II), allows the study of the polymers by EPR which provides a rich source of structural information [14].

This paper deals with the synthesis and characterization of a new series of potentially mesomorphic hydroxy-functionalized polyazomethines as shown in figure 1. The structural modifications affecting the repeating units depend on the monomeric diamine used in the polymer synthesis, and the influence of the central core of the repeating units on the polymer properties will be analysed. Both aliphatic and aromatic diamines were checked. Homopolyazomethines and copolyazomethines derived from terephthaldehyde and linear aliphatic diamines have been previously reported by Natansohn *et al.* [15–18] and exhibit mesomorphic behaviour. Taking into account these forerunners, the synthesis of polyazomethines derived from linear aliphatic diamines was accomplished (polymers 1–5). Obviously, *p*-substituted aromatic diamines give rise to rigid rod-like mesogenic units, but the melting transition is so high that no mesophase is observed before decomposition takes place. For this reason, lateral electron-donor substituents

(methoxy groups) were introduced (polymers 9 and 10), as well as a flexible ethylenic chain (polymer 6). The influence of diamines, which alter the coaxiality of the polymeric chains (polymer 8) or introduce kinks (polymers 7, 11 and 12), on the thermal transition will also be analysed. Furthermore, the two copolyazomethines shown in figure 2, containing a feed stock ratio of 1:1
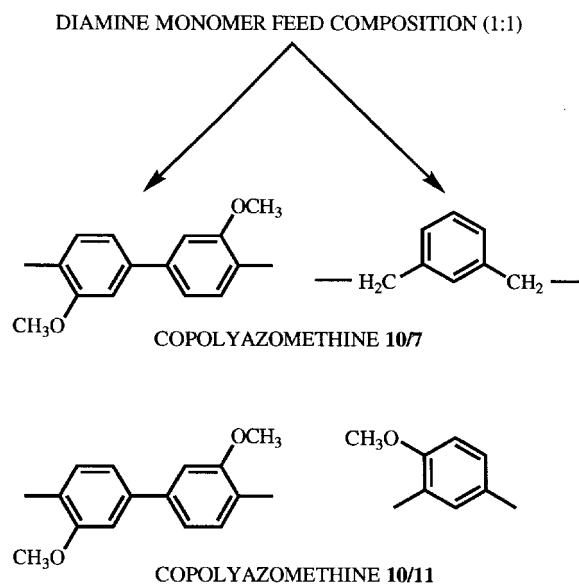

Figure 2. Central bridges derived from the diamines used in the synthesis of copolyazomethines (feed stock ratio of diamine monomers 1:1).

of premesogenic to non-mesogenic diamine monomer, were also synthesized. Together with the organic polyazomethines, some copper(II)-containing polymers were also synthesized by complexation of preformed polyazomethines derived from linear aliphatic diamine monomers, and the structural modifications introduced by copper(II)-complex formation were also analysed by EPR. These metal coordinated polyazomethines are coded as **n-Cu** where **n** represents the number of the methylene groups of the aliphatic diamine monomer.

2. Experimental
2.1. *Synthesis of the polymers*
The synthesis of the monomeric dialdehyde 1,10-bis(4-formyl-3-hydroxyphenoxy)decane has been described [4]. Most of the monomeric diamines were purchased commercially, and then purified by distillation under reduced pressure in the case of the aliphatic diamines and aliphatic–aromatic diamines, by sublimation in the case of 2,6-diaminopyridine, or by recrystallization from ethyl acetate/hexane in the case of 3,3′-dimethoxybenzidine. Alternatively, several diamines were obtained from the corresponding commercial salts (such as 2-methoxy-1,4-phenylenediamine sulphate hydrate, 4-methoxy-1,3-phenylenediamine sulphate hydrate and 2,2′-ethylenedianiline diphosphate) according to the following procedure: 0·023 mol of the salt was suspended in 300 ml of ether, and 0·0046 mol of 20 M NaOH was added with vigorous stirring. The mixture was stirred for 15 min, filtered to remove the inorganic salts and finally the ether was evaporated. The diamine was purified by distillation under reduced pressure in the case of 2,2′-ethylenedianiline or by recrystallization from ethyl acetate/hexane in the case of 2-methoxy-1,4-phenylenediamine and 4-methoxy-1,3-phenylenediamine. All the monomeric diamines were used immediately after purification and adequately protected from light.

The polyazomethines were synthesized according to the following method: 1·4 mmol of the appropriate diamine dissolved in the minimum volume of absolute ethanol (10–30 ml) was added to a three necked 250 ml flask provided with an inlet and outlet of nitrogen and containing a stirred solution of 1·4 mmol of 1,10-bis-(4-formyl-3-hydroxyphenoxy)decane in 110 ml of absolute ethanol and heated under reflux. 0·14 ml of glacial acetic acid was added immediately as a catalyst and the reaction mixture was heated under reflux and stirred for 4 h. After cooling, the polymer precipitate was filtered off and washed with a large amount of water and methanol. The product obtained was extracted in a Soxhlet apparatus with acetone for 24 h and dried under vacuum at 80°C with P_2O_5 for 24 h.

2.2. *Synthesis of the copper(II)-chelated polyazomethines*
A 0·44 mmol quantity of the appropriate, finely powdered polyazomethine was suspended in 20 ml of freshly distilled 1,4-dioxane, heated under reflux and stirred magnetically. Then 0·022 mmol of $(AcOCu)_2.2H_2O$ in 10 ml of hot 1,4-dioxane was added dropwise over 15 min. The suspension was heated under reflux with stirring under a nitrogen atmosphere for 2 h. After cooling, the reaction mixture was filtered and the solid washed with 1,4-dioxane, hot water and methanol. The polymer was dried under vacuum over P_2O_5 for 24 h at 80°C.

2.3. *Characterization techniques*
Elemental analysis was carried out with a Perkin-Elmer 240C microanalyser. The copper content was determined by inductively coupled plasma atomic emission spectroscopy (ICP-AES) using a Perkin-Elmer P-40 spectrometer. IR spectra were measured using KBr pellets and a Perkin-Elmer FTIR 1600. ^1H NMR measurements on polymer solutions were made with a Varian Unity-300 spectrometer operating at 300 MHz and using deuteriated trifluoroacetic acid as solvent. Fresh samples were used in order to avoid degradation. UV measurements were made using a UV-VIS spectrophotometer, KONTRON UVIKON-941, and polymeric films which were obtained by casting a 0·2–0·7% w/w polyazomethine solution in trifluoroacetic acid. After evaporating the solvent, the films were dried for 12 h under vacuum. Films were deprotonated by immersing in triethylamine/ethanol (1:1) for 4–5 h, washing them repeatedly with absolute ethanol and finally drying them under vacuum over P_2O_5 for 12 h.

The inherent viscosities of polyazomethines were measured at a concentration of 0·5 g dl^{-1} in methane sulphonic acid at 40°C using a Cannon–Fenske viscometer. Samples were used immediately after preparation to avoid degradation. When degradation was clearly detected, the longest efflux time was used to determine the inherent viscosity.

A Perkin-Elmer DSC-7 differential scanning calorimeter was used to determine the thermal transitions which were read at the peak maxima of the heating scan after annealing the sample for 1 h at a temperature below the melting transition. Glass transitions were measured at the midpoint of the heat capacity increase. The mesomorphic behaviour was confirmed by optical microscopy using a Nikon polarizing microscope fitted with a Mettler FP-82 hot stage and a Mettler FP-80 control unit. Thermogravimetric analysis was performed with an STD 2960 simultaneous DTA–TGA apparatus using powdered samples which were heated at 10°C min^{-1} under a nitrogen atmosphere.

The X-ray diffraction patterns were obtained with an evacuated Pinhole camera (Anton–Paar) operating with a point-focused Ni-filtered Cu Kα beam. Fibres were drawn from the mesomorphic melt with different thermal histories into air at room temperature by using preheated tweezers. Films were obtained from the mesomorphic melt by uniaxial shearing on a glass surface with the aid of a preheated Teflon bar. The samples were contained in Lindemann glass capillaries (0·7 mm diameter) and the diffraction patterns were collected on a photographic film.

EPR measurements were made at room temperature with a Bruker ESP-380 spectrometer working in the X-band. The powdered samples were examined by introducing them into standard EPR quartz tubes (707-SQ from Wilmad).

### 3. Results and discussion
3.1. *Synthesis and characterization of the polymers*

The polymers were obtained by condensation polymerization of the diamines and dialdehydes using the method depicted in the scheme in which ethanol is used as solvent and glacial acetic acid as catalyst. The method proved to be adequate for this kind of hydroxy-functionalized polyazomethine in spite of the fact that the polymers precipitate out of the polymerization media. In particular, polyazomethines derived from aliphatic diamines precipitate more quickly than those derived from aromatic diamines. The polyazomethines obtained generally show a good film and fibre forming ability [6]. However, and depending on the intended applications, the molecular weight can be increased by annealing at temperatures close to melting or in the molten state [1(b), 2]. Yields, elemental analyses, and selected spectral data for the polyazomethines are collected in tables 1 and 2. Polymers were isolated as powdered solids except in the case of polymer 11 which was isolated as a gum which becomes a brittle solid after extraction with acetone and drying. The colour of the polymers strongly depends on the extension of conjugation through the central bridge. Polyazomethines derived from aliphatic diamines are slightly yellow and those derived from aromatic diamines exhibit a deeper colouration (strong yellow or orange). Thin films of the polyazomethines were prepared to investigate the effects of the central core on the optical absorption and electronic structure of the materials. The lowest energy absorption maximum (λ_{max}) due to a $\pi \rightarrow \pi^*$ transition and the associated absorption edge (E_g) of the spectra for these films are collected in table 2. The protonic quaternization of the imine nitrogens of the polyazomethines (protonated films) causes a red shift of the electronic absorption spectra compared with the deprotonated films. The quaternization and complexation of imine nitrogens of polyazomethines have been reported as strategies to induce a high backbone planarity in addition to intramolecular hydrogen bonding. This argument may explain the observed red shift behaviour. However, the protonated films exhibit a relatively low environmental stability in comparison with fully aromatic polyazomethines. The switch from protonated to deprotonated state is monitored by a change in the colour intensity of the film.

Polymerization yields are high, in general higher than 85%, except in the case of polymer 12 which may be an indication of the low reactivity of the monomeric 2,6-diaminopyridine due to the electronegativity of the pyridinic nitrogen. This low reactivity is also reflected in the disagreement between the elemental analysis found and that calculated from the repeating unit.

These polyazomethines displayed a very low solubility in common organic solvents. They are soluble in strong
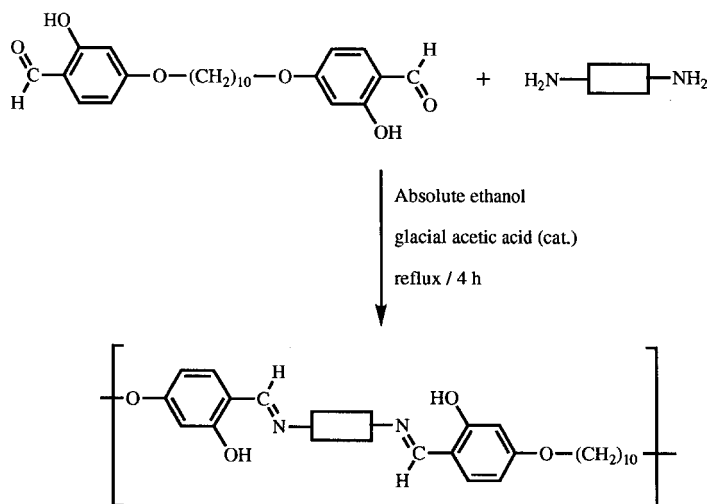
Scheme

Table 1. Yields and characterization data for the synthesized polyazomethines.

Polymer	Yield/%	% C calcd	% C found	% H calcd	% H found	% N calcd	% N found	$C=N$ (st) /cm^{-1}	$-CH=N-R$ δ/ppm
1	92	71·68	71·56	7·96	7·62	6·19	6·14	1626	8·29
2	93	72·10	72·07	8·15	8·34	6·01	6·29	1626	8·21
3	89	72·50	72·70	8·33	8·62	5·83	6·10	1627	8·22
4	97	72·87	72·70	8·50	8·87	5·66	5·61	1626	8·18
5	77	74·18	74·29	9·09	9·13	5·09	4·91	1625	8·18
6	97	74·70	74·35	7·39	7·25	5·44	5·25	1618 (sh), 1626	8·08, 8·69
7	93	74·70	74·75	7·39	7·62	5·44	5·47	1626	8·33
8	78	77·28	76·58	7·12	6·36	4·74	4·43	1613	8·22
9	91	72·09	71·74	6·98	6·98	5·43	5·41	1604	8·86, 8·80
10	81	73·30	72·81	6·75	7·05	4·50	4·53	1618	8·74
11	87	72·09	71·86	6·98	6·56	5·43	5·15	1604	8·76, 8·93
12	44	71·46	70·79	6·77	6·65	8·62	6·17	1631	9·43
10/7	80	73·90	73·42	7·04	6·45	4·93	4·83	1626	8·29, 8·75
10/11	85	72·75	72·52	6·85	6·99	4·92	4·83	1617	8·66, 8·76, 8·83

Table 2. The electronic absorption maxima (λ_{max}) and the absorption edges (E_g) for the synthesized polyazomethines.

Polymer	Protonated films λ_{max}/nm	Protonated films E_g/nm (eV)	Deprotonated films λ_{max}/nm	Deprotonated films E_g/nm (eV)
1	303, 340 (sh)	385 (3·22)	307	335 (3·70)
2	304, 339 (sh)	381 (3·26)	312	375 (3·31)
3	304, 342 (sh)	390 (3·18)	307	337 (3·68)
4	305, 338 (sh)	385 (3·22)	309	345 (3·60)
5	303, 341 (sh)	389 (3·19)	306	348 (3·57)
6	421	430 (2·89)	350	415 (2·99)
7	308, 345 (sh)	390 (3·18)	311	345 (3·60)
8	380	453 (2·74)	343	405 (3·06)
9	342, 420 (sh)	566 (2·19)	355	463 (2·68)
10	330, 500 (sh)	537 (2·31)	395	487 (2·55)
11	453	573 (2·17)	404	571 (2·17)
12	442	540 (2·30)	$\approx$350	503 (2·47)
10/7	438, 457 (sh), 494 (sh)	531 (2·34)	390	477 (2·60)
10/11	451	554 (2·24)	390	531 (2·34)

protonic acids such as trifluoroacetic acid or methane sulphonic acid, due to the protonation of the imine bond which diminishes the interactions between polymeric chains through electrostatic repulsions. ^{1}H NMR spectra and viscosity measurements were carried out in these solvents. However, acid-catalysed hydrolysis of the polymers in strong protonic acids may lead to degradation of the polymeric chains. For this reason, conclusions about molecular weight cannot be drawn with any accuracy from the ^{1}H NMR or η_{inh} data, but they are useful from a comparative point of view.

Azomethine bond formation during the polymerization was confirmed by FT-IR as is shown in table 1. The analysis for end groups did not reveal bands corresponding to amine or aldehyde groups. However, ^{1}H NMR analysis of the polyazomethines using deuteriated trifluoroacetic acid as solvent showed a signal corresponding to aldehyde terminal groups, and in the case of polyazomethines **1**–**7**, signals were also detected which can be attributed to the presence of amine end groups. Nevertheless, the effect of degradation of polymeric chains cannot be ruled out, especially in the case of these polyazomethines derived from aliphatic amines ($-CH_2-NH_2$) which quickly degrade in solution. Inherent viscosities were measured by using 0.5 g dl^{-1} solutions in methane sulphonic acid, and are collected in table 3. Data corresponding to polymers **1**–**5** are roughly calculated because of rapid degradation detected by a progressive decrease in the measured solution viscosity. However, taking into account this degradation and the structural differences among these polymers, the viscosimetric data provide information about the reactivity of the diamine monomers. Thus, polyazomethines derived from aliphatic or aliphatic–aromatic

Table 3. Inherent viscosities (η_{inh}) of the synthesized polyazomethines.

Polymer	η_{inh}	Observations
1	>1·07	fast degradation
2	>1·19	fast degradation
3	>0·93	fast degradation
4	>1·01	fast degradation
5	>0·80	fast degradation
6	0·89	
7	>1·00	partially soluble
8	0·18	
9	0·82	
10	0·98	
11	>0·44	partially soluble
12	>0·30	partially soluble
10/7	0·28	
10/11	>0·14	partially soluble

Table 4. Characterization data for the copper(II) complexed polyazomethines (**n-Cu**).

Polymer	% Cu calcd[a]	% Cu found[b]	% Cu introduced[c]	C=N (st) /cm^{-1}
3-Cu	10·99	3·76	34	1626
4-Cu	10·51	3·34	35	1625
5-Cu	10·09	4·10	40	1627
6-Cu	10·15	3·90	38	1625
10-Cu	8·86	3·54	40	1625

[a] Calculated % mol of coordinating sites complexed with copper(II) ions.
[b] % Mol of coordinating sites complexed with copper(II) ions obtained by ICP-AES.
[c] (Found/calculated) × 100.

Table 5. Thermal stabilities of the synthesized polyazomethines and the copper(II) complexed polyazomethines (**n-Cu**).

Polymer	TGA/°C[a]	DTGA[b]
1	326, 347	341, 426
2	324, 335	346, 422
3	329, 340	351, 420
4	328, 348	350, 426
5	340, 374	350, 440
6	346	364, 431
7	375	438
8	371	382
9	361	374, 441 (sh)
10	364	380, 438 (sh)
11	336	364, 430
12	361	411
10/7	291, 358, 406	316, 367, 440
10/11	354	369
3-Cu	324, 351	341, 422
4-Cu	325, 347	345, 424
5-Cu	325, 350	346, 414
6-Cu	321, 342	346, 422
10-Cu	332, 373	351, 440

[a] Thermogravimetric analysis: onset of the decomposition curve.
[b] Derivative thermogravimetric analysis: minimum of the derivative decomposition curve.

diamines (polymers **1**–**7**) showed a relatively higher η_{inh} which can be associated with the higher degree of polymerization reached by the more nucleophilic aliphatic amines. Furthermore, comparison of the η_{inh} of polymers **9** and **10**, derived from aromatic diamines containing electron-donor substituents, with that of the polyazomethine derived from 1,4-phenylenediamine ($\eta_{inh} = 0·41$) or 2-methyl-1,4-phenylenediamine ($\eta_{inh} = 0·45$) [4] makes evident the influence of the electronic character of the substituents in the diamine monomers. Higher degrees of polymerization are obtained by using aromatic diamines with electron-donor substituents. The low viscosity of polymer **8** can be understood in terms of the steric hindrance on the condensation step and the crankshaft topology introduced into the polymeric chain for the 2,2′-ethylenedianiline monomer.

The copper complexation of the polyazomethines derived from linear aliphatic diamines is easily accomplished using a THF suspension. The analysis of copper content reveals that only about 35–40% of the added copper ions react with the coordinating repeating units, as can be seen from table 4 which gives the characterization data for the copper-modified polyazomethines.

3.2. *Thermal stability*

The thermal stability of the polyazomethines and the copper(II) complexed derivatives was studied by simultaneous TGA–DTA under a nitrogen atmosphere. The experimental results are summarized in table 5.

All of the synthesized polyazomethines showed a good thermal stability, as is typical of this kind of polymer [19], and exhibited weight losses only at temperatures above 325–360°C. Furthermore, weight losses corresponding to solvent or volatile products were not detected at lower temperatures. The weight loss associated with thermal decomposition coincides with the decomposition peak observed in the DTA traces. Regarding the influence of structural modifications, polyazomethines derived from linear alkyl diamines (polymers **1**–**5**) exhibit lower decomposition temperatures. The length of the linear alkyl diamine seems to have no influence on the decomposition temperatures, except in the case of polymer **5** which exhibits a relatively high thermal stability. Moreover, two decomposition processes are clearly observed for this kind of polymer. The derived copper-complexed polyazomethines **n-Cu** ($n = 3, 4, 5, 6$ and 10) exhibit a similar thermal stability to the parent polymers. The introduction of phenyl rings increases the

thermal stability. Polymers **9** and **10** exhibit lower thermal stability than polyazomethines derived from 1,4-phenylenediamine (TGA = 388°C) or benzidine (TGA = 406°C) [4] as a consequence of the introduction of oxygen-containing lateral substituents.

3.3. *DSC measurements and mesomorphic behaviour*

On the first heating, DSC traces of the as-synthesized polyazomethines displayed wide peaks typical of polydisperse samples and corresponding to multiple endothermic transitions which generally disappear in the second and successive heating scans or after annealing the sample at temperatures close to melting. For this reason, most of the polymeric samples were subjected to a similar thermal history by annealing for one hour at a temperature close to melting in order to characterize the melting transition. This annealing temperature was selected by analysing the first DSC scan and selecting a temperature approximately 20°C below the onset temperature of the melting transition. Table 6 collects the phase transition temperatures assigned by DSC and the optical microscopy observations.

The mesogenicity of these polyazomethines strongly depends on the geometry of the calamitic repeating unit. However, the rigidity of the central core is not a critical

condition for obtaining liquid crystalline polyazomethines as was shown by Natashon *et al.* [15–18] who prepared mesomorphic polymers derived from terephthaldehyde and several aliphatic diamines. In particular, the polyazomethine derived from terephthaldehyde and 1,10-diaminodecane has been reported to show a crystal smectic G phase. Similar behaviour was observed for polyazomethines with shorter spacers. They showed liquid crystalline phases which have not been identified, mainly because they are too unstable. However, the polymers **1**–**5** synthesized from linear aliphatic diamines did not show mesophases. The same behaviour was previously reported for the polyazomethine derived from 1,2-diaminoethane [4]. The flexibility of the aliphatic diamine part prevents the central core from being rigid enough, in spite of the intramolecular H-bond rings. The molecular geometry is determined by the possibility of rotation about the C–C bonds in the flexible central group, and only a few conformers have an adequate rod-like structure for exhibiting liquid crystallinity. Presumably, the energy barrier among 'rod-like' conformers and 'bent' conformers is not high enough at temperatures above T_m and consequently an isotropic phase is observed. As is shown in table 6 the melting temperatures of these polymers decrease as the length

Table 6. DSC and optical microscopic observations of the synthesized polyazomethines and the copper(II) complexed polyazomethines (**n-Cu**).

Polymer	Annealing[a] /°C	T_m/°C[b]	T_i/°C[b]	Mesophase	T_g/°C[b]
1	110	162	—	—	39
2	155	192	—	—	—
3	100	145	—	—	—
4	100	169	—	—	—
5	100	133, 142	—	—	—
6	225	273	318	nematic	—
7	130	148, 152	—	—	42
8	150	208	—	—	—
9	150	167	295 (dec)	nematic	70
10	150	193	325 (dec)	nematic–smectic[d]	57
11	[c]	—	—	—	91
12	130	135, 148, 162	—	—	—
10/7	140	156	[e]	nematic	48
10/11	100	124	[e]	nematic	80
3-Cu		141	—	—	66
4-Cu		189	—	—	—
5-Cu		—	—	—	67
6-Cu		150	—	—	31
10-Cu		136	—	—	—

[a] Annealing temperature of samples annealed for 1 h at a temperature below melting as determined during the first heating scan.
[b] Thermal transitions characterized by DSC on a heating scan at a scanning rate = 10°C min^{-1}: T_m = melting transition temperature read at the maximum of the endothermic peak; T_i = isotropization transition temperature read at the maximum of the endothermic peak; T_g = glass transition determined as the midpoint of the heat capacity jump.
[c] Sample annealed at 70°C for 12 h.
[d] See text for explanation.
[e] No peak corresponding to isotropization was observed. Decomposition is detected at temperatures higher than 315°C.

of the flexible aliphatic segment increases following an alternating odd–even sequence. The rigidity of the polymeric chains can be altered by metal complexation in order to induce mesogenicity. The induction of liquid crystalline phases by transition metal complexation in non-mesogenic *N*-alkylated poly(ethyleneimine)s has been previously reported by Ringsdorf and co-workers [20]. The complexation of the aliphatic polyazomethines with a low percentage of copper(II) gives rise to a relative decrease of the melting temperature in comparison with the parent polyazomethines, but the melt is highly viscous and isotropic in nature.

Polyazomethine **6** derives from the aromatic–aliphatic diamine 2-(4-aminophenyl)ethylamine, which gives rise to a repeating unit containing two aromatic rings linked by an imine bond. The corresponding polyazomethine, derived from ethylenediamine, is non-mesogenic in spite of having a relatively high rigidity. In consequence, the introduction of the aromatic ring in polymer **6** seems to be critical for the appearance of a mesophase. Thus, rigid units consisting of at least two aromatic rings linked by an azomethine bond and with a linear geometry, are responsible for the mesomorphic properties of these materials.

The diamine monomer used in the synthesis of polymer **7** disrupts the conjugation through the azomethine bond and introduces flexibility and kinks in the polymeric chains which disturb the appearance of mesomorphic phases. However, the polymer exhibits a relatively low melting temperature, similar to those of the aliphatic polyazomethines **3** and **5**, but has a higher thermal stability. For this reason, this diamine was selected for copolymerization with a diamine which promotes mesogenicity, in order to study the influence on the thermal transitions and mesogenic properties (see below). In the case of polyazomethine **8**, the azomethine bond extends the conjugation, but the rigid unit is not mesogenic due to the steric hindrance introduced by the *ortho*-ethylene connecting group. These groups have a relatively low flexibility and consequently, the repeating units have a rigid-crankshaft geometry, which alters the coaxiality of the polymeric chains, similarly to the polyazomethine derived from 1,5-diaminonaphtalene ($T_m = 216°C$; $T_i = 308°C$), but the high molecular width and the non-coplanar disposition of the aromatic rings prevents the appearance of a mesophase. Furthermore, this polyazomethine exhibits a high melting transition and was rejected for copolymerization.

Rigid and linear polyazomethines derived from *p*-phenylenediamine and benzidine exhibited a high melting point and decomposed before a mesophase could be observed [4]. The introduction of lateral groups disturbed the intermolecular interactions and decreased the melting temperature without having a noticeable effect

on the linearity of the rigid central core. Thus, the lateral methoxy groups in position 2- of *p*-phenylenediamine (polymer **9**) and 3,3′- of benzidine (polymer **10**) have a remarkable effect on the melting temperature. Both polymers melt into a nematic mesophase at temperatures below 200°C and exhibit a low tendency to crystallize on cooling the anisotropic melt, giving rise to a mesomorphic glass. When we use 4-methoxy-1,3-phenylenediamine (polymer **11**) instead of 3-methoxy-1,4-phenylenediamine (polymer **10**), an amorphous material is obtained and the mesomorphic properties disappear as a consequence of the disruption of the linearity or kink introduced by the *meta*-substitution. A similar tendency was previously reported for the polyazomethine derived from *m*-phenylenediamine, although that polymer is semi-crystalline. Polymer **12** is also derived from a *meta*-substituted diamine, and exhibits a low T_m. However, the low reactivity of the 2,6-diaminopyridine rules out this monomer as a good candidate for copolymerization.

In order to check the efficiency of copolymerization on decreasing the melting temperatures, whilst maintaining mesogenicity, two different copolymers were synthesized by using 3,3′-dimethoxybenzidine as promesogenic monomer and 1,3-di(aminomethyl)benzene or 4-methoxy-1,3-phenylenediamine as non-mesogenic monomer in a feed stock ratio of 1 : 1. The composition of the polymer approximately corresponds to the feed stock composition as confirmed by ^{1}H NMR. Both copolymers exhibit a decrease of the melting temperature with respect to the homopolymer (polymer **10**), and melt into a mesophase which extends over a broad range of temperature. On cooling the anisotropic melt no crystallization was observed.

One of the most remarkable characteristics of these mesogenic polyazomethines, especially in the case of polymers **9** and **10** and the copolyazomethines, is the tendency to increase their melt viscosity on heating. This behaviour is related to the proclivity of this type of polymer to increase the molecular weight on heating as we have previously confirmed for very similar hydroxy-functionalized polyazomethines [4, 6]. The textures exhibited by the mesomorphic homo- and co-polymers were not easy to recognise by polarizing light microscopy due to the highly viscous nature of the melt for most of the polymers. In particular, polymers **6** and **9** and the copolymers exhibited a highly viscous granular texture in the mesophase which converts to a marbled texture by mechanical stress. These textures can be assigned as nematic in comparison with previously described polyazomethines. Polymer **10** melts into a relatively low viscosity mesophase which exhibits defined threaded textures which can be assigned to a nematic mesophase. Figure 3(*a*) shows the texture of the sample observed at
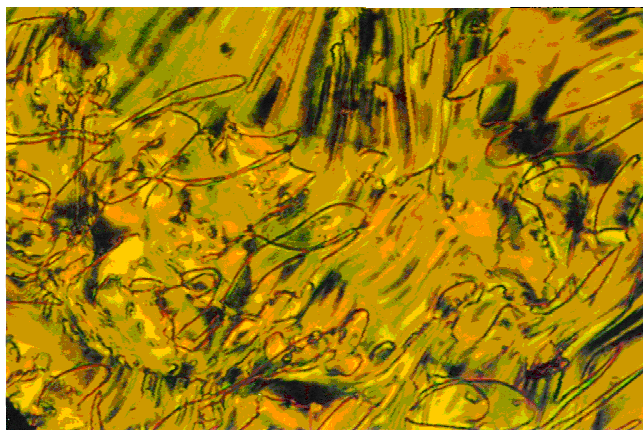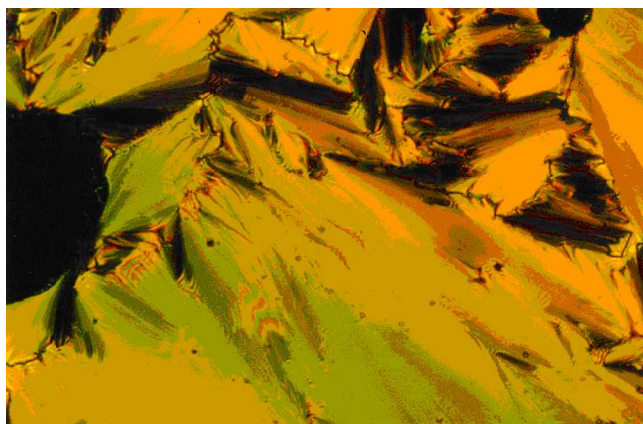
Figure 3. Polarized light micrographs of polymer **10** at 225°C. (*a*) Sample without annealing; (*b*) sample annealed for 15 h.

225°C. However, an evolution of the texture is observed on annealing the polymer. Figure 3 (*b*) corresponds to the same sample after annealing at 225°C for 15 h and shows a broken fan-shaped texture. This type of texture is typical of a smectic mesophase and suggests that the initial nematic mesophase becomes smectic on annealing. A study by optical microscopy showed that the change occurs after annealing for more than 1 h. However, well defined textures require longer annealing periods. This behaviour was not observed for the rest of polyazomethines of this series.

3.4. *X-ray diffraction measurements*

In order to confirm the nature of the mesophases shown by the polymers and with the aim of obtaining information about their structures, X-ray diffraction measurements were performed on selected samples of the mesogenic polyazomethines. In particular, the homopolymers **9** and **10** and the copolymer **10/11** were examined. In these three cases, X-ray photographs of

the fibres drawn from the mesomorphic melt were taken. For polymer **10**, films and powdered samples were also examined in order to gain more information on the structural changes that take place when the polymer is annealed at the mesophase temperature.

Fibres drawn from the mesomorphic melt showed a high degree of orientation which was revealed by the low degree of arcing (polar angular spreading) of the scattered maxima for all the polymers studied. In figure 4, the fibre pattern of polymer **9** is shown as an example. The monomeric units are oriented along the stretching direction. In the patterns, there are two basic features to be observed: (1) the maxima at small angles, located in the meridian region, and (2) the wide-angle crescents located in the equatorial region. Both sets of maxima are diffuse, which is consistent with the nematic nature of the mesophase assigned by optical microscopy. The small angle spots are reinforced at each side of the meridian; this suggests the existence of short range smectic C-like order in the nematic phase (skewed cybotactic domains). The presence of this four-point pattern indicates that the layer normal in the smectic C fluctuations is tilted against the molecular axes and the layers are distributed on the surface of a cone whose axis is parallel to the director. The measured thicknesses *d* of the smectic C-like layers are gathered in table 7. The four-point splitting is specially noticeable for polymer **9** (see figure 4), and this allows an estimation of the tilt angle in the cybotactic regions ($\alpha = 36°$), as well as of the apparent molecular length ($l = 31$ Å).

It is interesting to compare the experimentally found layer thickness *d* with the length of the repeating unit *L* calculated from Dreiding stereomodels assuming a fully-extended structure of the molecules (carbon–carbon
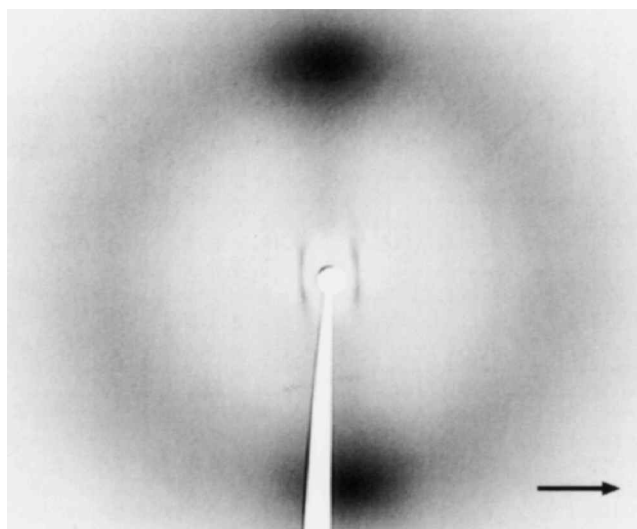

Figure 4. X-ray diffraction pattern of a fibre extruded from the mesomorphic melt of polymer **9**.

Table 7.   X-ray diffraction data for the fibres drawn from the nematic melts of polyazomethines **9** and **10** and copolyazomethine **10/11**. d: measured layer spacing in the cybotactic regions (± 0.5 Å); D: measured mean intermolecular distance (± 0.1 Å); L: repeating unit length estimated from Dreiding stereomodels (± 1 Å).

| Polymer	d/Å	D/Å	L/Å
9	25	4·1	32
10	33	4·0	36
10/11	29·5	4·0	36/31

single bonds and carbon–nitrogen double bonds in the all-*trans*-conformation). In the three polymers studied, the measured layer thickness d is smaller than the calculated molecular length L, which is expected because of the molecular tilting (see table 7). In the case of polymer **9**, the apparent molecular length, either deduced directly from the diffraction pattern (measured from the component of the scattering vector parallel to the director) or estimated as $l = d/\cos \alpha = 25 \text{Å}/0.809 = 31 \text{Å}$, is in good agreement with the calculated value $L = 32 \text{Å}$ (the estimated error for the experimental measurement at small angles is ± 0.5 Å and for the length calculated from Dreiding stereomodels is ± 1 Å). Moreover, a length of 30·76 Å has been measured in the crystalline phase for the fully-extended repeating unit of a very similar polyazomethine (the only difference from polymer **9** is the presence of a methyl lateral group instead of the methoxy group) [6]. This indicates that the repeating unit of polymer **9** in the mesophase is predominantly in the all-*trans*-conformation.

From the wide angle crescents, an estimation can be made of the mean intermolecular lateral separation D (see table 7). In the three polymers studied this distance (4·0–4·1 Å) is shorter than that usually found in low- and high-molecular mass mesogens (D about 4·5 Å) [21]. This suggests high molecular interactions in our polymers which may well be connected with intermolecular hydrogen bonding between hydroxyl groups and oxygen or nitrogen atoms, in addition to the intramolecular hydrogen bonding between the *ortho*-hydroxyl group and the nitrogen atom in the azomethine bond. This is consistent with the low tendency of fibres of these polyazomethines to fray, [6, 22] and accounts for the deduced all-*trans*-conformation, as the closeness of the molecular axes must force the hydrocarbon chains to adopt an extended structure.

In addition to the small angle maxima and the wide angle crescents, the fibre patterns display a set of equidistant diffuse bands at middle and wide angles in the meridian region (see figures 4 and 5). These lines have been previously observed in other X-ray patterns of nematic phases and have been accounted for by the existence of short range linear correlations between the mesogenic cores. In particular, in another main chain polymer [23], the phenomenon was assigned to the presence of uncorrelated rows of equally spaced moieties formed by several repeating units.

A detailed study of the mesophase of polymer **10** was carried out in order to elucidate the structural changes which are involved in the texture changes observed by optical microscopy in this compound. With this aim, X-ray patterns were taken by using oriented samples as fibres or films obtained from the mesomorphic melt at 225°C without annealing or after being annealed for 1, 2 or 3 h. In addition, non-oriented powdered samples with the same thermal history as the oriented samples were also studied. In all cases, the patterns of the unannealed samples are unambiguously characteristic of a nematic phase containing skewed cybotactic domains, as has been described above for the fibres. This is shown by the breadth and diffuseness of the small angle scattering (see figure 5(a)). On the other hand, in the patterns of the annealed samples, the small angle spots, characteristic of the interlayer order, are progressively sharper and stronger (see figure 5(b)). This suggests that the correlation length of the smectic C-like domains extends over longer distances. This effect is noticeable even after only one hour of annealing at 225°C, and can be interpreted as a slow isothermal transition from a nematic mesophase to a smectic mesophase. Apart from the sharpening and strengthening of the small angle peaks, no other structural modifications are observed on annealing at 225°C. Thus, the structural parameters (interlayer spacing d, intermolecular mean distance D) are unaffected, and this supports the view that the smectic mesophase obtained is of the C type. From this point of view, the continuous transition from the nematic to the smectic phase in polymer **10** would consist of an increase in the size of the correlated regions in which a change from a local order to a long range ordered structure takes place. This isothermal transition, not usually found in liquid crystals, could be accounted for by the reactivity in the nematic molten state of these polymeric chains containing mesogenic units with four conjugated aromatic units. This reactivity gives rise to an increase in the degree of polymerization and a reorganization of the mobile polymeric chains to arrange in a smectic structure. The increase in degree of order of the liquid crystalline phase with molecular mass has been previously described for liquid crystal polymers by studying different samples which differ in average molecular mass and molar mass distribution [24]. This phenomenology is ascribed to an increase of the cooperativity between distant units belonging to the same macromolecular backbone mediated by the orientational field of the liquid crystalline order [24(b)].
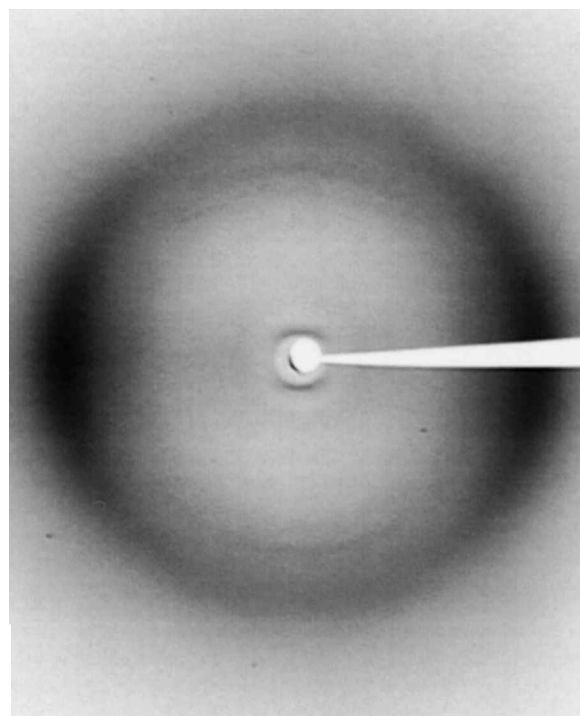
(*a*)
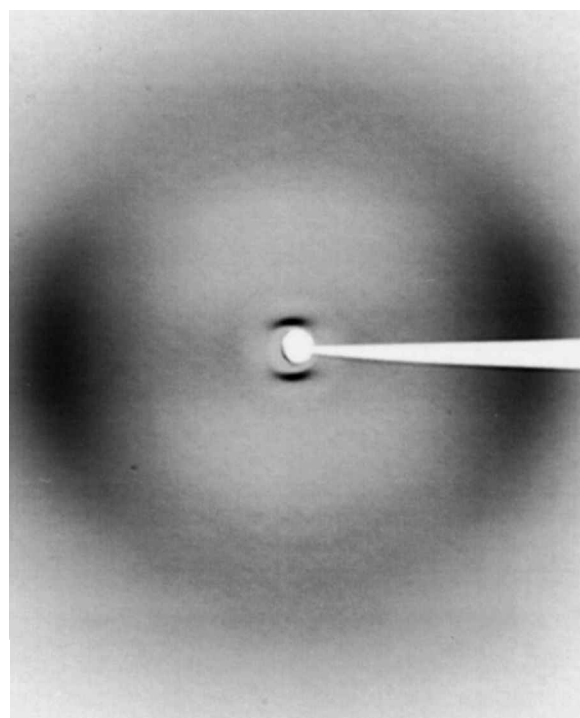
(*b*)

Figure 5. X-ray diffraction patterns of powder samples of polymer **10**. (*a*) Sample heated to the mesomorphic state at 225°C and quenched to room temperature; (*b*) sample annealed in the mesomorphic state at 225°C for 2 h and quenched to room temperature. Some preferential orientation was detected.

3.5. *Microstructural study of copper(II)-complexed polymers by EPR*

As mentioned above, the non-mesomorphic polyazomethines derived from linear aliphatic diamines were complexed with paramagnetic copper(II) ions to investigate the possible induction of liquid crystalline behaviour. The copper(II) salicylaldimine complex formation might give rise to two effects (see figure 6). Firstly, the metal ion can be coordinated to two separate repeating units (figure 6(*a*)). In this case, the repeating unit acts as a bidentate ligand and an interchain coordination takes place, giving a crosslinked material. Secondly, a bending of the polymeric chain could occur by intrachain complexation of the metal ion with a tetradentate repeating unit (figure 6(*b*)). Both possibilities have been previously reported for similar polyazomethines [13, 14]. Thus, polyazomethines derived from ethylenediamine, 1,5-naphthalenediamine and 1,4-phenylenediamine and the same dialdehyde monomer were synthesized and complexed with different amounts of copper(II) ions in order to check the kind of coordination they exhibit. EPR spectra of the polymers proved that intrachain coordination takes place in the case of the polyazomethine derived from ethylenediamine and an interchain coordination for the others derived from aromatic diamines. The logical explanation of this behaviour arises from the flexibility of the ethylenic central bridge compared with the rigid aromatic rings.

We have studied the copper complexed polymers **n-Cu** in which the length of the chain of the aliphatic diamine used in the synthesis has been increased from 3 to 6 and 10, in order to analyse the structural changes introduced by the copper(II) ions (interchain or intrachain coor-
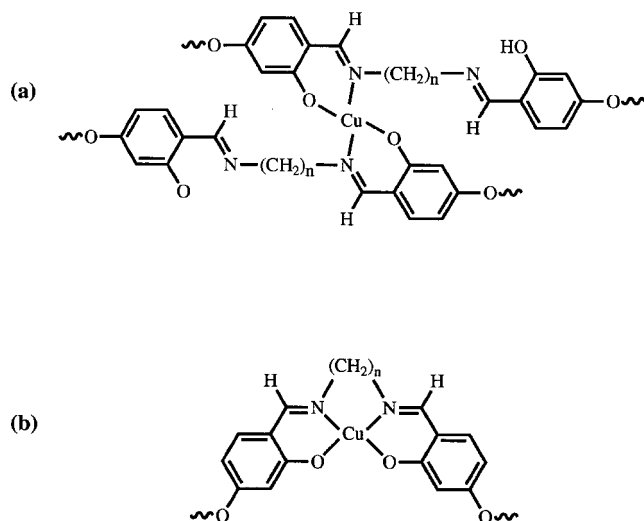

Figure 6. Modifications introduced into the polymeric chains by copper(II) complexation of polyazomethines derived from aliphatic diamines (**n-Cu**).

dination). The EPR spectra of **n-Cu** ($n = 3$, 4, 5, 6 and 10) samples were measured at room temperature. Figure 7 displays these spectra of the copper complexes compared with that derived from complexed polyazomethine obtained from 1,2-ethylenediamine ($n = 2$) and previously reported [13, 14]. In all these cases, the spectrum can be assigned to a Cu(II) entity in an almost square-planar environment and some divergence in the low field region associated with parallel entities are clearly resolved. These spectra can be described with an axial spin Hamiltonian including the electronic Zeeman (characterized by $g_\parallel$ and $g_\perp$) and hyperfine (given by $A_\parallel$ and $A_\perp$) contributions. In spite of the fact that copper has two naturally occurring isotopes ([63]Cu in 69·2% and [65]Cu in 30·8% with a very close nuclear *g* factor [63]g_n/[65]$g_n = 0·94$) the hyperfine lines of both species are not resolved in the spectra.

The spectra of all the polymers **n-Cu** ($n = 3$, 4, 5, 6 and 10) coincide, whereas there are marked differences on comparing with the spectrum of the polyazomethine derived from ethylenediamine ($n = 2$). The parallel features are centred at a higher field and hyperfine splitting is larger in this case than in those of **n-Cu** with $n = 3$, 4, 5, 6 and 10.

These results are summarized in table 8 which shows the values obtained for $g_\parallel$ and $A_\parallel$ in all the complexed polymers compared with those corresponding to complexed polyazomethines derived from 1,5-naphthalenediamine and ethylenediamine as previously

Table 8. EPR parameters for previously synthesized copper(II) containing polyazomethines and those corresponding to the copper(II) complexed polyazomethines (**n-Cu**) derived from aliphatic diamines.

Polymer	$g_\parallel$	$A_\parallel$
NP[a]	2·22	521
ED = 2-Cu[b]	2·20	594
n-Cu (n = 3, 4, 5, 6, 10)	2·22	530

[a] Polyazomethine derived from 1,5-naphthalenediamine [14].
[b] Polyazomethine derived from ethylenediamine [14].

reported. The hyperfine coupling constants correspond to the average value among the two isotopes of copper.

As can be observed in table 8, values obtained for $g_\parallel$ and $A_\parallel$ in the case of polymers derived from aliphatic diamines, $H_2N-(CH_2)_n-NH_2$ when $n \geqslant 3$, are similar to those obtained for the polymers derived from 1,5-naphthalenediamine. These relate to an interchain coordination and differ from those obtained for the polymer derived from ethylenediamine, which gives an intrachain coordination. Consequently, a predominant interchain coordination, and therefore crosslinking of polymeric chains, takes place. Some authors have previously reported the synthesis and properties of several coordination polymers of copper, nickel, cobalt and manganese derived from different polyazomethines [25–29]. However, the stereochemistry of these complexes has not been generally characterized in depth [30] in spite of the fact that intrachain coordination has been traditionally suggested for salicylaldimine derived polymers, independently of the diamine used in the polymer synthesis.

4. Conclusions

A series of hydroxy functionalized polyazomethines has been synthesized by acid-catalysed solution polycondensation of commercial diamines and a dialdehyde which contains a decamethylenic flexible spacer. Polymers were obtained in good yields except in the case of polymer **12**. The polymers have a tendency to increase in molecular mass on heating and exhibit a good film- and fibre-forming ability. All the samples are of good thermal stability, especially polymers derived from diamine monomers containing aromatic rings. The presence of oxygen-containing substituents decreases the thermal stability.

Thermal transitions and mesogenic properties were studied by DSC and optical microscopy; only polymers containing at least two aromatic rings conjugated through an azomethine bond and having a linear geometry exhibit a mesomorphic phase. The presence of lateral substituents decreases T_m and allows the observation of the mesophase over a wide range of temperatures.
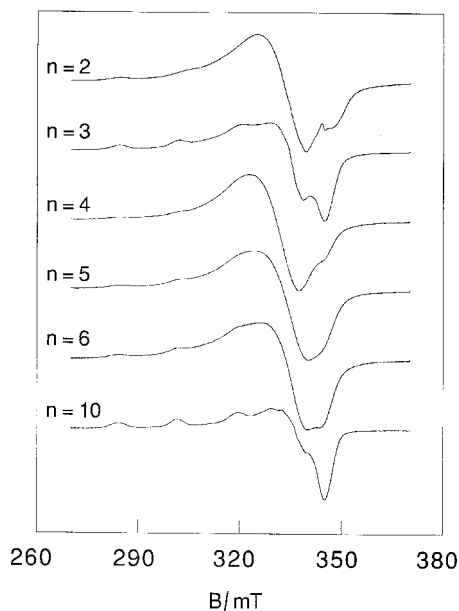

Figure 7. EPR spectra of the copper(II) complexed polyazomethines derived from aliphatic diamines (**n-Cu**). EPR spectrum of the copper(II) complexed polyazomethine derived from ethylenediamine ($n = 2$), previously reported [14] is included as reference.

The introduction of kinks (polymers **11** and **12**) or a strong alteration of the coaxiality (polymer **8**), as well as the introduction of flexible aliphatic central bridges, prevents the appearance of anisotropic melts. Copolymerization of pre-mesogenic monomers with non-mesogenic monomers in a 1:1 composition yields mesomorphic materials with a relatively low T_m.

The nature of the observed mesophase was studied by polarizing optical microscopy and X-ray diffraction. Despite the poorly defined textures observed by optical microscopy, the mesophase can be identified as nematic in nature. Fibres obtained from the mesomorphic melt showed a pattern consistent with a nematic melt with cybotactic S_C domains. In the case of polymer **10**, an evolution from a nematic into a smectic C-like mesophase was observed by optical microscopy and X-ray diffraction on annealing the sample in the mesophase temperature range.

Finally, the presence of *ortho*-hydroxyl groups allows the complexation of polymeric chains. This polymer reaction was carried out with the polyazomethines derived from aliphatic diamines and the structural modification introduced by the metal (copper II) studied by EPR. A predominant interchain coordination, which gives rise to crosslinking, was observed in all samples.

References

[1] See, e.g. (*a*) JENEKHE, S. A., and YANG, C. J., 1991, *Chem. Mater.*, **3**, 985; (*b*) YANG, C. J., and JENEKHE, S. A., 1995, *Macromolecules*, **28**, 1130 and references therein.

[2] (*a*) MORGAN, P. W., PLETCHER, T. C., and KWOLEK, S. L., 1983, *Polym. Prep.*, **24**, 470; (*b*) MORGAN, P. W., KWOLEK, S. L., and PLETCHER, T. C., 1987, *Macromolecules*, **20**, 729; (*c*) WOJTKOWSKI, P. W., 1987, *ibid.*, **20**, 740.

[3] See, e.g. (*a*) JENEKHE, S. A., JOHNSON, P. O., and AGRAWAL, A. K., 1989, *Macromolecules*, **22**, 3216; (*b*) JENEKHE, S. A., and JOHNSON, P. O., 1990, *ibid.*, **23**, 4419; (*c*) YANG, C. J., and JENEKHE, S. A., 1991, *Chem. Mater.*, **3**, 878.

[4] BARBERÁ, J., ORIOL, L., and SERRANO, J. L., 1992, *Liq. Cryst.*, **12**, 37.

[5] (*a*) MELÉNDEZ, E., and SERRANO, J. L., 1983, *Mol. Cryst. Liq. Cryst.*, **91**, 173; (*b*) ELGUERO, J., JAIME, C., MARCOS, M., MELÉNDEZ, E., SÁNCHEZ-FERRANDO, F., and SERRANO, J. L., 1987, *J. mol. Struct.*, **150**, 1; (*c*) CHUDGAR, N. K., and SHAH, A., 1993, *Liq. Cryst.*, **14**, 1163.

[6] CERRADA, P., ORIOL, L., PIÑOL, M., SERRANO, J. L., IRIBARREN, I., and MUÑOZ-GUERRA, S., 1996, *Macromolecules*, **29**, 2515.

[7] LEWTHWAITE, R. A., GOODBY, J. W., and TOYNE, K. J., 1994, *Liq. Cryst.*, **16**, 299.

[8] CHEN, C. T. and SUSLICK, K. S., 1993, *Coord. Chem. Rev.*, **128**, 293.

[9] HÄRTEL, M., KOSSMEHL, G., MANECKE, G., WILLE, W., WÖHRLE, D., and ZERPNER, D., 1973, *Angew. makromol. Chem.*, **29/30**, 307.

[10] See, e.g. DE LOHRAY, B. B., SIVARAM, S., and DHAL, P. K., 1994, *Macromolecules*, **27**, 1291.

[11] HAASE, W., GRIESAR, K., ISKANDER, M. F., and GALYAMETDINOV, Y., 1993, *Mol. Mater.*, **3**, 115.

[12] LONG, N. J., 1995, *Angew. Chem. int. Ed. Engl.*, **34**, 21.

[13] ALONSO, P. J., MARTÍNEZ, J. I., ORIOL, L., PIÑOL, M., and SERRANO, J. L., 1994, *Adv. Mater.*, **6**, 663.

[14] ORIOL, L., ALONSO, P. J., MARTÍNEZ, J. I., PIÑOL, M., and SERRANO, J. L., 1994, *Macromolecules*, **27**, 1869.

[15] NATANSOHN, A., YANG, H., and CLARK, C., 1991, *Macromolecules*, **24**, 5489.

[16] YANG, H., and NATANSHON, A., 1992, *Macromolecules*, **25**, 5331.

[17] YANG, H., and NATANSHON, A., 1992, *Macromolecules*, **25**, 5798.

[18] YANG, H., and NATANSHON, A., 1993, *Polymer*, **34**, 4135.

[19] HU, L. C., and CHANG, T. C., 1990, *J. Polym. Sci. A, Polym. Chem.*, **28**, 3625.

[20] FISCHER, H., PLESNIVY, T., RINGSDORF, H., and SEITZ, M., 1995, *J. chem. Soc., chem. Commun.*, 1615.

[21] NOËL, C. 1985, *Polymeric Liquid Crystals*, edited by A. Blumstein (Plenum Press), p. 53.

[22] CERRADA, P., ORIOL, L., PIÑOL, M., and SERRANO, J. L., (in preparation).

[23] ALONSO, P. J., PUÉRTOLAS, J. A., DAVIDSON, P., MARTÍNEZ, B., MARTÍNEZ, J. I., ORIOL, L., and SERRANO, J. L., 1995, *Macromolecules*, **26**, 4304.

[24] See, e.g. (*a*) BLUMSTEIN, R. B., STICKLES, E. M., GAUTHIER, M. M., BLUMSTEIN, A., and VOLINO, F., 1984, *Macromolecules*, **17**, 177; (*b*) LAUS, M., ANGELONI, A. S., SPAGNA, A., GALLI, G., and CHIELLINI, E., 1994, *J. mater. Chem.*, **4**, 437.

[25] PATEL, M. N., and JANI, B. N., 1985, *J. macromol. Sci-Chem.*, **A22**, 1517.

[26] BOTTINO, F. A., FINOCCHIARO, P., LIBERTINI, E., MAMO, A., and RECCA, A., 1983, *Polym. Commun.*, **24**, 63.

[27] PATEL, M. N., PATIL, S. H., and SETTY, M. S., 1981, *Angew. makromol. Chem.*, **97**, 69.

[28] SAWODNY, W., RIEDERE, M., and URBAN, E., 1978, *Inorg. Chim. Acta*, **29**, 63.

[29] MANECKE, G., and WILLE, E., 1970, *Makromol. Chem.*, **133**, 61.

[30] PATEL, M. N., and PATIL, S. H., 1983, *J. macromol. Sci-Chem.*, **A19**, 201.